MICROCOPY RESOLUTION TEST CHART

NATIONAL BUREAU OF STANDARDS-1963-A

REPORT DOCUMENTATION PAGE

1a. REPORT SECURITY CLASSIFICATION Unclassified		1b. RESTRICTIVE MARKINGS		
2a. SECURITY CLASSIFICATION AUTHORITY		3. DISTRIBUTION/AVAILABILITY OF REPORT Approved for public release; distribution unlimited.		
2b. DECLASSIFICATION/DOWNGRADING SCHEDULE				
4. PERFORMING ORGANIZATION REPORT NUMBER(S)		5. MONITORING ORGANIZATION REPORT NUMBER(S) 23474.16-MS		
6a. NAME OF PERFORMING ORGANIZATION Colorado School of Mines Center for Welding Research	6b. OFFICE SYMBOL (If applicable)	7a. NAME OF MONITORING ORGANIZATION U. S. Army Research Office		
6c. ADDRESS (City, State, and ZIP Code) Golden, Colorado 80401		7b. ADDRESS (City, State, and ZIP Code) P. O. Box 12211 Research Triangle Park, NC 27709-2211		
8a. NAME OF FUNDING/SPONSORING ORGANIZATION U. S. Army Research Office	8b. OFFICE SYMBOL (If applicable)	9. PROCUREMENT INSTRUMENT IDENTIFICATION NUMBER DAAL03-86-K-0064		
8c. ADDRESS (City, State, and ZIP Code) P. O. Box 12211 Research Triangle Park, NC 27709-2211		10. SOURCE OF FUNDING NUMBERS		

10. SOURCE OF FUNDING NUMBERS			
PROGRAM ELEMENT NO.	PROJECT NO.	TASK NO.	WORK UNIT ACCESSION NO.

11. TITLE (Include Security Classification)

The Nature of Metallurgical Reactions in Underwater Welding

12. PERSONAL AUTHOR(S)
S. Ibarra, D.L. Olson, C.E. Grubbs

13a. TYPE OF REPORT	13b. TIME COVERED FROM _____ TO _____	14. DATE OF REPORT (Year, Month, Day) April, 1987	15. PAGE COUNT 6

16. SUPPLEMENTARY NOTATION
The view, opinions and/or findings contained in this report are those of the author(s) and should not be construed as an official Department of the Army position, policy, or decision, unless so designated by other documentation.

17. COSATI CODES			18. SUBJECT TERMS (Continue on reverse if necessary and identify by block number)
FIELD	GROUP	SUB-GROUP	

19. ABSTRACT (Continue on reverse if necessary and identify by block number)

Thy pyrometallurgical reactions are characterized as a function of depth for underwater wet welding. The influence of weld metal compositional variations with depth on weld metal microstructures are described. Metallurgical suggestions as to compositional modifications to underwater wet welding electrodes to achieve the desired microstructure and properties are given.

DTIC
ELECTE
SEP 1 1 1987
D
A

20. DISTRIBUTION/AVAILABILITY OF ABSTRACT ☐ UNCLASSIFIED/UNLIMITED ☐ SAME AS RPT. ☐ DTIC USERS	21. ABSTRACT SECURITY CLASSIFICATION Unclassified	
22a. NAME OF RESPONSIBLE INDIVIDUAL D.L. Olson	22b. TELEPHONE (Include Area Code) 303-273-3787	22c. OFFICE SYMBOL

DD FORM 1473, 84 MAR   83 APR edition may be used until exhausted.   SECURITY CLASSIFICATION OF THIS PAGE
All other editions are obsolete.   UNCLASSIFIED

OTC 5388

The Nature of Metallurgical Reactions in Underwater Welding

by S. Ibarra, Amoco Corp.; C.E. Grubbs, Global Divers & Contractors Inc.; and D.L. Olson, Colorado School of Mines

ABSTRACT

The pyrometallurgical reactions are characterized as a function of depth for underwater wet welding. The influence of weld metal compositional variations with depth on weld metal microstructure are described. Metallurgical suggestions as to compositional modifications to underwater wet welding electrodes to achieve the desired microstructure and properties are given.

INTRODUCTION

Underwater welding has been recognized as a difficult and a potentially cost saving engineering task that becomes more important with the maintenance of existing marine structures. Masubuchi et. al. (1,2), Dadian (3), Magarajan and Loper (4), Hart (5) and Inglis and North (6) have reviewed the technologies, characterized the difficulties, and discussed the limitations of underwater welding. Specifications for underwater welding which describe the mechanical requirements that load bearing weld deposits must meet are available (12). Christensen et. al. (7-10) have introduced basic concepts for underwater weld metal chemistry and metallurgy. Their research was primarily on the influence of pressure on hyperbaric shielded metal arc weld metal compositions. Christensen's work (7) did suggest that similar weld metal compositional variations should occur in wet underwater welding. Madator (11) reported on the influences of parameters on the welding process and on the metallurgical reactions.

Christensen et. al (7-10) have shown that with increasing pressure or depth that weld metal manganese and silicon substantially decreased. The weld metal manganese experienced a 0.3 wt. pct. decrease from the surface composition at 30 bars (1000 ft.). Weld metal silicon decreased 0.10 wt. pct. with an increase of 8 bars or 250 ft. depth. Weld metal oxygen and carbon contents increase by factors greater than two when comparing composition of hyperbaric welds made at 1000 ft. to weld metal made on the surface. This manganese and carbon variation can cause significant change in hardenability of the weld metal. The weld metal

oxygen went from an acceptable 300 ppm to a very questionable 750 ppm level. High weld metal oxygen has been related to inferior weld metal toughness (15). Mathisen and Gjermundsen (14) reported similar variations for weld metal manganese and silicon for wet welds made down to 70 meters. They also found little variation in carbon for the depth range that they investigated.

There is a major difference between wet and hyperbaric welding. Both experience increase pressure with depth (one bar for each 10 meter increase in depth), but the wet environment also influences the cooling rate during welding which affects the nature of the weld metal phase transformation. Wet underwater welding also introduces hydrogen into the welding arc and into the weld metal.

Olson and Ibarra (13) addressed the influence of these compositional variations on the weld metal phase transformation and microstructure. They used metallurgical concepts, such as shifts in the continuous cooling transformation (CCT) diagram, as an instructional procedure to understand how the environmental factors of hydrostatic pressure will change weld metal microstructure and thus the weld metal properties. Increases in weld metal oxygen and silicon should promote weld metal inclusions and better nucleation conditions for weld metal ferrite. This effectively moves the C-shaped CCT curves to shorter times. Increases in weld metal manganese and carbon will increase weld metal hardenability and thus move the C-shaped CCT curves to longer times. The trends for underwater welding of increased weld metal oxygen and carbon and decreased weld metal manganese and silicon makes it difficult to determine the final shape and position of nucleation curves on the CCT diagram. Olson and Ibarra (13) suggested the use of a weld metal oxygen-effective weld metal manganese (Mn+6C) diagram to predict weld metal microstructure with these complex compositional variations. With the diagram it is possible to predict the necessary compositional modifications of the underwater wet welding electrode as a function of depth.

87 9 9 193

The present underwater wet welding investigation was designed to characterize weld metal made by welding at depths down to 100 meters (325 feet) and to test the metallurgical concepts and analytical procedure suggested by Olson and Ibarra (13). In this investigation wet welds were made by Shielded Metal Arc welding (SMAW) down to a depth of 100 meters (325 ft.). These wet welds were thoroughly analyzed for microstructural and compositional variations. The mechanical properties were also determined.

EXPERIMENTAL PROCEDURES

Shielded Metal Arc 1/8 inch diameter E6013 welding electrodes were coated for underwater wet welding by Global Divers and Contractors Inc. The same batch of these coated E6013 underwater welding electrodes were used in preparing weld specimens at the surface, 2m (7 ft.), 10m (33 ft.), 30 m (90 ft.), 50 m (160 ft.) and 100 m (325 ft.). The welding parameters were 28-37 volts and 135-150 amperes with a travel speed of 6 to 11 inches per minute. DC straight polarity was used for all welding.

A 0.50 inch thick low carbon ASTM A-36 steel plate was used for these welding experiments. A single V edge preparation with a backing plate was used as shown in Figure 1. Approximately 15 stringer bead passes were used to fill the edge preparation and make an acceptable weld deposit.

The weld metal composition was analyzed. At least three weld metal specimens were measured for each element at each depth. The weld metal manganese, silicon, chromium, nickel, molybdenum, aluminum and vanadium was measured using an ARL emission spectrometer. Weld metal oxygen, nitrogen, carbon and sulfur were analyzed with Leco combustion interstitial analyzers.

The weld metal microstructure was analyzed after metallographic preparation and by careful point count to determine the amount of grain boundary (primary) ferrite, side plate (Widmanstatten) ferrite, acicular ferrite and ferrite with aligned carbides (upper bainite). Mechanical properties were measured and found to be acceptable according to the requirements of ANSI/AWS D3.6-83 for type B welds (12).

RESULTS AND DISCUSSION

The weld metal compositions were measured for the weld deposits made at specific depths down to 100 meters (325 ft.). The weld metal manganese contents as a function of depth are given in Figure 2. Notice the sharp decrease in manganese content from 0.6 wt. pct. for the surface weld to 0.25 wt. pct. for the weld made at 30 meters (90 ft.). This decrease in weld metal manganese content can be directly correlated to the rapid increase in weld metal oxygen content for the same range of depth as seen in Figure 3. This suggests the manganese content is controlled by oxidation. Similar decreases in weld metal content were found for the weld metal silicon as shown in Figure 2. It would be expected that these oxide forming elements would respond in this manner to this increase in oxygen.

The weld metal carbon content was found to have a major increase from the weld made at the surface to

the welds from 50 meter (160 ft.) as shown in Figure 4. Such an increase in both carbon and oxygen for hyperbaric SMA welds as a function of pressure (depth) has been related by Grong et. a. (9) to be associated with the carbon monoxide reaction. The carbon monoxide is assumed present in the welding arc due to the decomposition of carbonates in the electrode covering. Grong et. al. (9) found that their weld metal carbon and oxygen contents related to the law of mass action for the carbon monoxide reaction, that is,

$$CO(g) = \underline{C} = \underline{0} \qquad \text{(eq. 1)}$$

and the equilibrium constant, K, is approximately equal to

$$K = \frac{[C][0]}{P_{CO}} \qquad \text{(eq. 2)}$$

The partial pressure of carbon monoxide, P_{CO}, is related to the total pressure, P, through Dalton's Law;

$$P_{CO} = X_{CO} P \qquad \text{(eq. 3)}$$

where X_{CO} is the fraction of the welding arc atmosphere that is carbon monoxide. Substituting and rearranging the equations 2 and 3, the product of the weld metal carbon, [C] and weld metal oxygen [0] is then given by:

$$[C][0] = KX_{CO}P = k'P \qquad \text{(eq. 4)}$$

where k' is a constant. Grong et. al. (9) found a linear relationship between this [C][0] product and the total pressure, P, or depth for the SMA hyperbaric welding. To evaluate whether the same carbon monoxide reaction is controlling in wet underwater welding the [C][0] product for these wet underwater welds was also plotted as a function of depth (pressure). An excellent linear correlation was found for the weld metal carbon and oxygen product results up to 50m (160 ft.) as shown in Figure 5. This suggests the carbon monoxide reaction is controlling the oxygen content up to 50m (160 ft.) and this oxygen content controls the oxidation of the manganese, silicon, chromium, and vanadium and thus their weld metal contents.

For depths greater than 50 meters (160 ft.) the weld metal oxygen and carbon become fairly constant down to at least 100 meters (325 ft.). Notice also that the weld metal manganese and silicon content are also fairly constant between 50 and 100 meters. This suggests that the oxygen content controls the weld metal manganese and silicon contents but the carbon monoxide reaction is not controlling at depths somewhat greater than 50 meters.

278

The compositional results for greater than 50 meters (160 ft.) suggest that the following H_2O decomposition reaction may be controlling:

$$H_2O(g) = H_2(g) + \underline{O} \qquad \text{(eq. 5)}$$

The law of mass action for this reaction is given by:

$$K_2 = \frac{P_{H2}[O]}{P_{H2O}} \qquad \text{(eq. 6)}$$

where K_2 is the equilibrium constant for the above H_2O decomposition reaction (eq. 5), PH_2 is the partial pressure of hydrogen and P_{H2O} is the partial pressure of water. Using Dalton's law:

$$P_{H2O} = X_{H2O}P \qquad \text{(eq. 7)}$$

$$P_{H2} = X_{H2}P \qquad \text{(eq. 8)}$$

where X_{H2O} is the fraction of water and X_{H2} is the fraction of hydrogen in the weld arc. Substituting and rearranging the above equations, the following equations results:

$$K_2 = \frac{X_{H2}P[O]}{X_{H2O}P} = \frac{X_{H2}}{X_{H2O}}[O] \qquad \text{(eq. 9)}$$

From equation (9) it can be seen that the weld metal oxygen content would remain constant. This constant weld metal oxygen content is similar to the results found to depths greater than 50 meters.

The weld metal microstructure was analyzed by optical metallography. The quantitative analysis was performed at 500X magnification with 1000 point counts. The microstructure of the top as-deposited weld bead was measured for all specimens. This procedure of investigating only the top bead was to eliminate any influence of the multiple pass welding thermal cycle on the weld metal microstructure. The mechanical properties normally obtained from testing weld metal relate to the total weld deposits which is made up of microstructures from various reheated zones. The relative amounts of each ferrite morphology was measured and reported in Figure 6. Notice the shift in the relative amounts of the three ferrite morphologies. At depths near the surface the weld metal is mainly primary ferrite with 10 to 20 pct. upper bainite. With increasing depth the relative amount of primary ferrite decreases to about 50 percent with increasing amounts of upper bainite and side plate ferrite. The major changes in microstructure occur in the first 50 meters (160 ft.) in depth just as with the weld metal composition. At depths greater than 50 meters the weld metal composition and microstructure remains fairly constant. The microstructure directly responds to the variation in weld metal composition.

In this investigation, three ferrite morphologies were found and are primary grain boundary ferrite, upper bainite, and side plate (Widenstatten) ferrite. It would have been more desirable to have formed some acicular ferrite which promotes excellent toughness instead of the significant side plate ferrite content. The side plate has a similar lath formation mechanism as acicular ferrite but differs in that it nucleates on the existing grain boundary ferrite and grows into the remaining austenite. Whereas, acicular ferrite nucleates on intragranular inclusions under specific conditions. Olson and Ibarra (13) have suggested the desirability of achieving high acicular ferrite contents in underwater welds. This is possible but only with specific weld metal alloying additions, such as titanium and boron with the proper weld metal oxygen and manganese contents.

The E6013 electrode used in this investigation did not produce the desired weld metal composition to form acicular ferrite and side plate ferrite resulted. Figure 7 is a schematic CCT diagram indicating the nucleation curves for the various ferrite morphologies and their positions to explain the microstructural changes as a function of pressure or depth.

The increase in the amount of side plate ferrite with increasing depth suggests that an increase in the weld metal carbon content with increasing depth promoted greater hardenability and moved this C-shaped curve of the CCT diagram to longer times. The carbon influence counteracted the reduction in weld metal manganese content and the increase in weld metal oxygen content.

Notice the position of the side plate ferrite relative to the acicular ferrite on this schematic CCT diagram. It suggests that with increasing hardenability, such as adding manganese that the curves can be sufficiently moved to longer time to form some amount of acicular ferrite.

A weld metal oxygen content versus effective weld metal manganese content (Mn+6C) diagram has been suggested (13) to assist in selecting compositional modifications for underwater wet welding consumables. A diagram for the deposit of a underwater wet E6013 electrode is shown in Figure 8. This diagram was constructed based on the microstructural and compositional analysis from this investigation and represents a cooling rate typically found in wet welding in the Gulf of Mexico. Notice that this diagram suggests that to achieve the desired acicular ferrite that increases in both weld metal oxygen and manganese are required.

CONCLUSIONS

1. The wet underwater weld metal manganese and silicon contents decrease with depth down to a specific depth and stabilize to constant content with further increasing in depth.

2. The wet underwater weld metal oxygen and carbon contents increase with depth down to a specific depth and then remain fairly constant with further increasing depth.

3. In wet underwater welding, the carbon monoxide decomposition reaction controls

the oxygen content down to approximately 50 meters and oxygen content controls the weld manganese and silicon contents at all depths by oxidation reactions.

4. The wet underwater weld metal microstructures were correlated schematically to cooling rates and weld metal composition through predictive diagrams.

5. Modification in the composition of underwater wet welding consumables to achieve desired microstructure and properties can be guided by the use of a predictive diagram.

ACKNOWLEDGEMENT

REFERENCES

(1) Chong-Liang Tsai and K. Masubachi, "Interpretive Report on Underwater Welding", WRC Bulletin 224, pp. 1-37, WRC, New York, NY (1977).

(2) R. T. Brown and K. Masubuchi, "Fundamental Research on Underwater Welding", Welding Journal 54 (6), 178s-188s (1975).

(3) M. Dadian, "Review of Literature on the Weldability Underwater of Steels", Welding in the World 14 (3/4), pp. 80-99 (1976).

(4) V. Nagarajan and C. R. Loper, "Underwater Welding of Mild Steel: A Metallurgical Investigation of Critical Factors", Offshore Technology Conference, Houston, paper OTC2668, May (1976).

(5) P.H.M. Hart, "The Potential Weldability Problems in Underwater Welding Offshore Engineering Materials", Underwater Welding for Offshore Installations, pp. 9-14, Welding Institute, Cambridge, UK 1977).

(6) M. R. Inglis and T. H. North, "Underwater Welding: A Realistic Assessment", Welding and Metal Fabrication 47 (4), 165-178 (1979).

(7) N. Christensen, "The Metallurgy of Underwater Welding", Underwater Welding, pp. 71-94, IIW Conference, Trondheim, Norway, Pergamon Press (1983).

(8) N. Christensen and K. Gjermundsen, "Effect of Pressure on Weld Metal Chemistry", IIW Doc. IX-212-384-76 (1976), supplement IIW Doc. II-212-395 (1977, American Delegation, AWS, Miami, FL.

(9) O. Grong, D. L. Olson, and N. Christensen, "On the Carbon Oxidation in Hyperbaric MMA Welding", Metal Construction 17 (12), pp. 810R-814R (1985).

(10) N. Christensen, "The Metallurgy of MMA Hyperbaric Welding", IIW Doc. IIA-596-83 (1984).

(11) N. M. Madator, "Influence of the Parameters of the Underwater Welding Process on the Intensity of Metallurgical Reactions", Welding Research Abroad (3), p. 63 (1972).

(12) American Welding Society, "Specification for Underwater Welding", ANSI/AWS D3.6-83, Miami, FL (1983).

(13) D. L. Olson and S. Ibarra, "Underwater Welding Metallurgy", First OMAE Specialty Symposium on Offshore and Arctic Frontiers, ASME, New York, NY, pp. 439-447 (1986).

(14) U. Mathisen and K. Gjermundsen, "Undervannssveising", SINTEF Rep. STF16 F79049, Trondheim, Norway (1979).

(15) T. H. North, H. B. Bell, A. Koukabi, and I. Craig, "Notch Toughness of Low Oxygen Content Submerged Arc Deposits", Welding Journal 58 (6), pp. 343A-353A (1979).
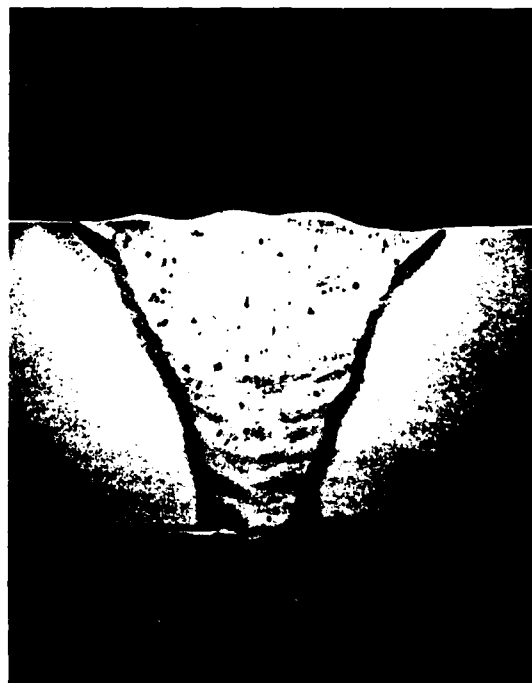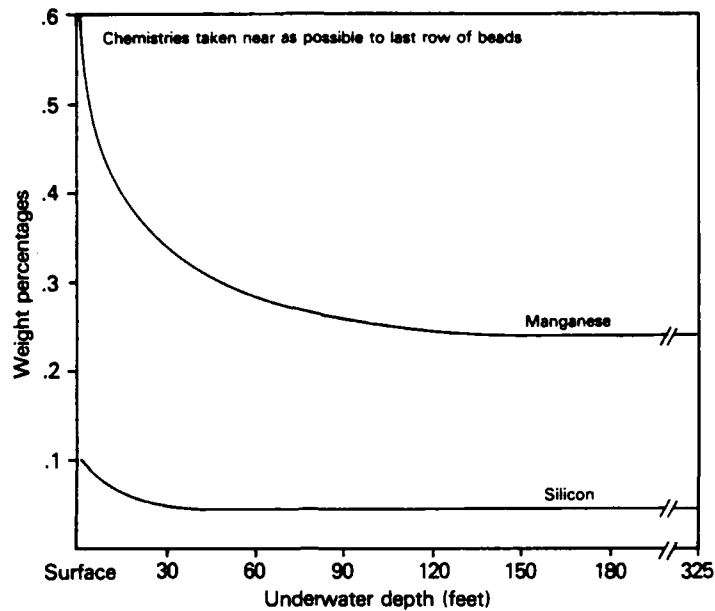
Fig. 1—Cross section of underwater wet weld.

Fig. 2—Wet underwater weld metal manganese and silicon as a function of depth.
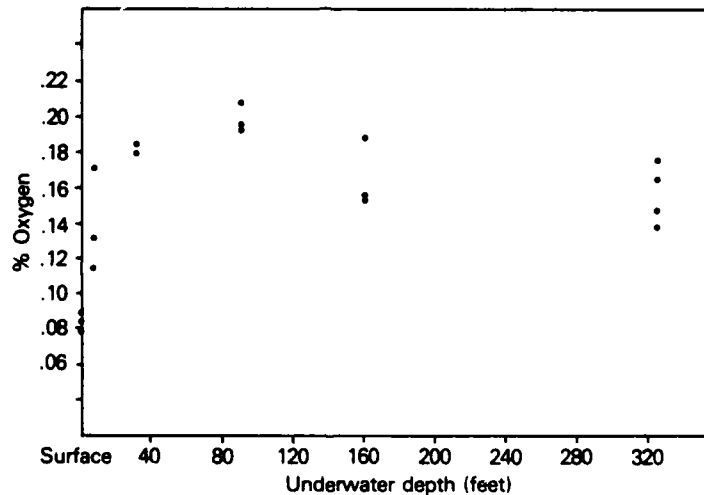

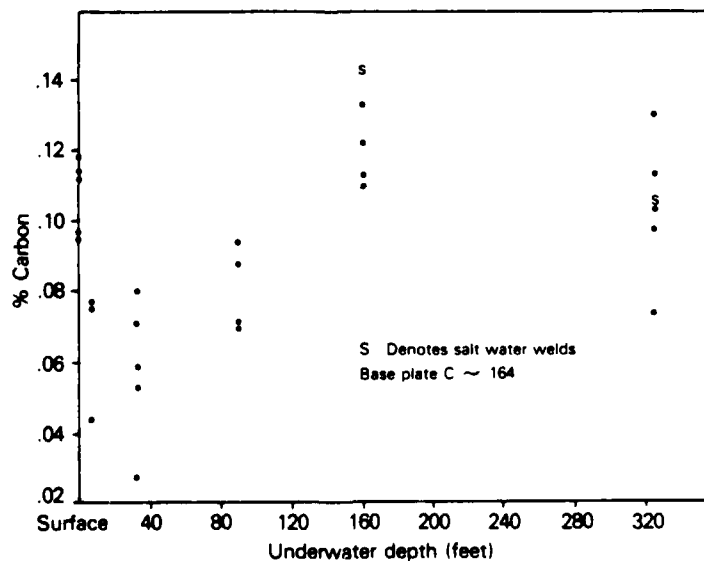Fig. 3—Wet underwater weld metal oxygen as a function of depth.
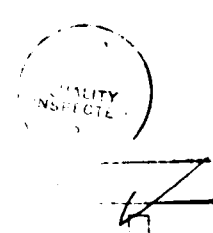

S   Denotes salt water welds

Base plate C ~ 164

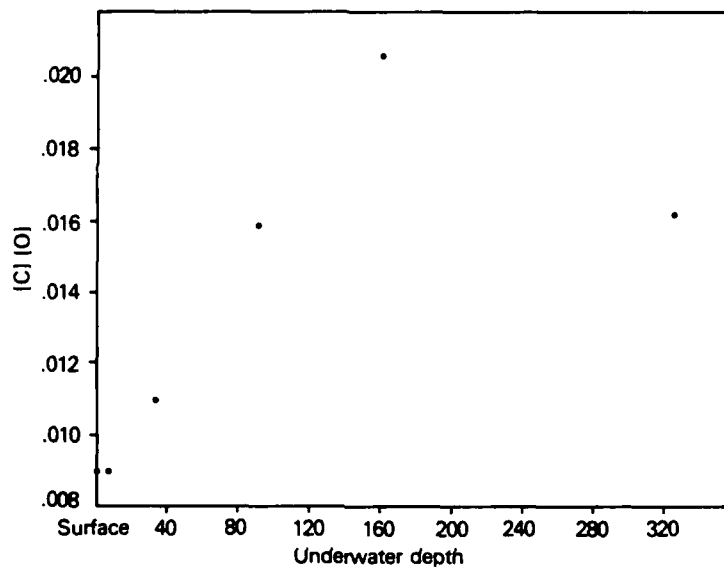Fig. 4—Wet underwater weld metal carbon as a function of depth
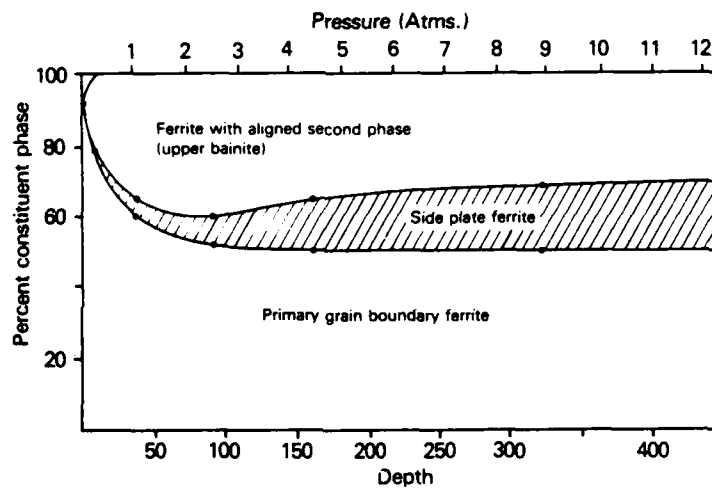
Fig. 5—Product of [C]·[O] vs. depth.

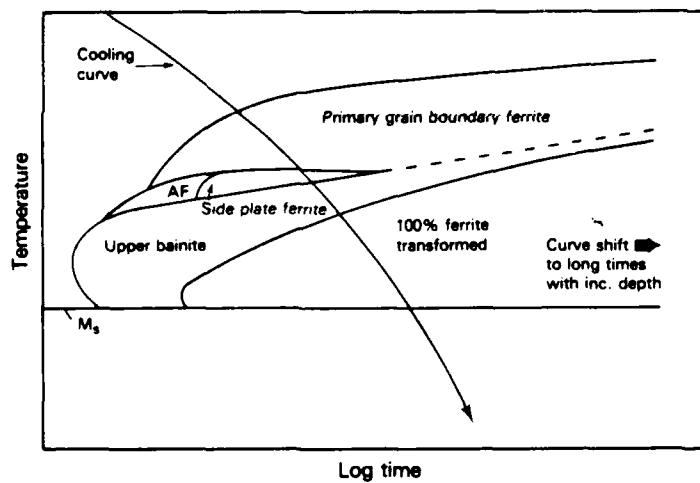Fig. 6—Weld metal constituent phases as a function of depth.

Fig. 7—Continuous cooling transformation curves for underwater welds.
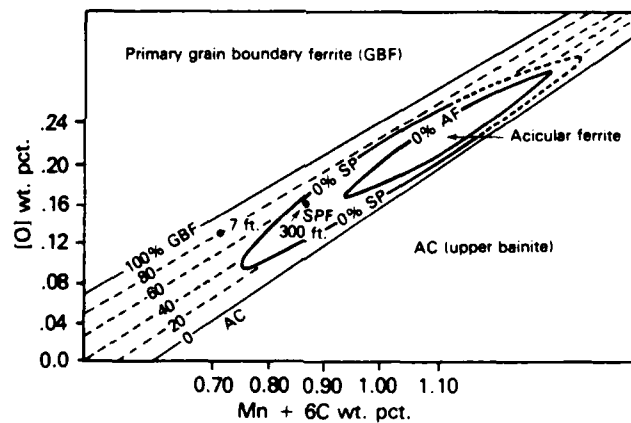

Fig. 8—Weld metal oxygen content vs. weld metal hardenability.

END

10-87

DTIC